Journal of Solid State Chemistry **159,** 209–214 (2001)
doi:10.1006/jssc.2001.9181, available online at http://www.idealibrary.com on IDEAL®

Inorganic-Organic Hybrid Materials: Synthesis and Structure of a Reduced Ferrous Molybdophosphate, $[(C_{12}H_8N_2)_3Fe^{II}]_2[Fe^{II}Mo^{V}_{12}(H_2PO_4)_6(PO_4)_2(OH)_6O_{24}]$, in the Presence of Fe(II)(1,10-Phenanthroline)$_3$ Complex

Yun-Shan Zhou,*,† Li-Juan Zhang,* Xiao-Zeng You,* and Srinivasan Natarajan†

*Coordination Chemistry Institute and State Key Laboratory of Coordination Chemistry, Nanjing University, Nanjing 210093, P. R. China; and †Chemistry and Physics of Material Unit, Jawaharlal Nehru Centre for Advanced Scientific Research, Jakkur P.O., Bangalore 560064, India

Received November 2, 2001; in revised form March 12, 2001; accepted March 26, 2001

A new composite solid of the formula $[(C_{12}H_8N_2)_3Fe^{II}]_2[Fe^{II}Mo^{V}_{12}(H_2PO_4)_6(PO_4)_2(OH)_6O_{24}]$ 1 has been synthesized from a reaction mixture of MoO_3, $Fe_2(C_2O_4)_3 \cdot 6H_2O$, $C_2H_2O_4 \cdot 2H_2O$, 1,10-phenanthroline monohydrate, H_3PO_4, and H_2O under hydrothermal conditions. Crystal data: trigonal, space group $R\bar{3}$, $a = 16.874(6)$ Å, $c = 30.117(7)$ Å, $V = 7426(4)$ Å^3, $R_1 = 0.0190$, w$R_2 = 0.0468$, and $S = 1.137$. The structure of 1 is built up from $FeMo_{12}(H_2PO_4)_6(PO_4)_2(OH)_6O_{24}^{4-}$ cluster anions connected to each other via hydrogen bonds. The arrangement of clusters is such that each cluster is surrounded by six equivalent anions resulting in three-dimensional cavities. The charge balancing cation, $[(C_{12}H_8N_2)_3Fe]^{2+}$ complex, resides in the cavities and interact with the clusters through hydrogen bonds. There is also strong π–π interactions exist among the phenyl rings. © 2001 Academic Press

INTRODUCTION

Metal oxide-based inorganic/organic hybrid solid phases have received considerable interests due to their wide structural diversities and versatile applications in catalysis, sorption, energy storage and optical and magnetic materials (1–4). The evolution of metal oxide chemistry, on the other hand, is dependent on the synthesis of new solids possessing unique structures and properties, although the synthesis of such compounds by rational design remains elusive. Typical examples are the cooperative assembly of organic components and transition metal oxides including vanadium oxides (5–7), molybdenum oxides (8, 9), reduced molybdenum phosphates (10, 11), iron phosphates (12, 13), iron molybdenate (14), etc. To date, however, there is a relative paucity of structural data known for inorganic–organic systems incorporating two octahedrally coordinated transition elements due to the lack of suitable synthetic methods. Recently, it has been demonstrated that hydrothermal techniques are ideally suited for the preparation of these novel solids (15–19). In this paper, the synthesis and structure of the first discrete ferrous molybdophosphate constructed from reduced ferrous molybdophosphate matrix and Fe(II)(1,10-phenanthroline)$_3$ complex, $[(C_{12}H_8N_2)_3Fe]_2[FeMo_{12}(H_2PO_4)_6(PO_4)_2(OH)_6O_{24}]$, **1**, is presented.

EXPERIMENTAL SECTION

The title compound is synthesized by employing hydrothermal methods. In a typical synthesis, a mixture of MoO_3 (0.2 g), $Fe_2(C_2O_4)_3 \cdot 6H_2O$ (0.23 g), $C_2H_2O_4 \cdot 2H_2O$ (0.19 g), 1,10-phenanthroline monohydrate (0.08 g), H_3PO_4 (0.37 ml, 85%) and H_2O (8 ml) were taken in the mole ratio of 3.5:1.2:3.7:1:13.9:300. The mixture was placed in a 23-ml PTFE-lined acid digestion bomb at 180°C for 72 h. After cooling to room temperature, black blocks of **1** were obtained. Anal. Calc. For $C_{72}H_{66}Fe_3Mo_{12}N_{12}O_{62}P_8$: H, 1.4; C, 23.8; N, 4.6. Found: H, 1.1; C, 24.5, N, 4.2. The presence of $C_2H_2O_4 \cdot 2H_2O$, is necessary to reduce the Mo^{6+} present in the starting materials and to prevent the formation of the familiar Keggin type heteropolymolybdates (19).

A suitable single crystal was carefully selected under a polarizing microscope and glued to the tip of a glass fiber using cyanoacrylate (super glue) adhesive. Single crystal structure was performed on a CAD4SDP4 four-circle single crystal X-ray diffractometer with graphite-monochromated Mo$K\alpha$ radiation using $\omega/2\theta$ scans. The unit cell was determined from the setting angles of 25 well-centered reflections over the range $11^\circ < 2\theta < 13^\circ$. Three standard reflections were measured every hour, which showed no appreciable variation during the course of data collection. Data were corrected for Lorenz and polarization effects and for absorption using the azimuthual scans (20). Relevant details of the structure determination are presented in Table 1.

0022-4596/01 $35.00

TABLE 1
Crystal Data and Structure Refinement Parameters for, 1, $[(C_{12}H_8N_2)_3Fe^{II}]_2[Fe^{II}Mo^{V}_{12}(H_2PO_4)_6(PO_4)_2(OH)_6O_{24}]$

Empirical formula	$C_{72}H_{66}Fe_3Mo_{12}N_{12}O_{62}P_8$
Formula weight	3657.96
Temperature	293(2) K
Wavelength	0.71073 Å
Crystal system, space group	Trigonal, *R*-3
Unit cell dimensions	$a = 16.874(6)$ Å, $\alpha = 90^\circ$ $b = 16.874(6)$ Å, $\beta = 90^\circ$ $c = 30.117(7)$ Å, $\gamma = 120^\circ$
Volume	7426(4) Å^3
Z, Calculated density	3, 2.454 Mg/m^3
Absorption coefficient	2.136 mm^{-1}
F(000)	5338
Crystal size	$0.2 \times 0.2 \times 0.2$ mm
Theta range for data collection	1.55° to 25.01°
Limiting indices	$-20 \le h = 20$, $-15 \le k \le 20$, $-35 \le l \le 24$
Reflections collected/unique	9062/2908 [*R*(int) = 0.0254]
Completeness to theta = 25.01	99.7%
Absorption correction	ψ-Scan
Max. and min. transmission	0.72 and 0.64
Refinement method	Full-matrix least-squares on F^2
Data/restraints/parameters	2908/2/299
Goodness-of-fit on F^2	1.137
Final *R* indices [$I > 2\sigma(I)$]	$R^a = 0.0190$, w$R_2^b = 0.0468$
R indices (all data)	$R^a = 0.0269$, w$R_2^b = 0.0491$
Largest diff. peak and hole	0.404 and −0.503 e Å^{-3}

[a] $\sum(|F_o - F_c|)/\sum|F_o|$.
[b] $[\sum w(|F_o^2 - F_c^2|)/\sum[w|F_o^2|^2]]^{1/2}$.

TABLE 2
Atomic Coordinates ($\times 10^4$) and Equivalent Isotropic Displacement Parameters (Å$^2 \times 10^3$) for 1, $[(C_{12}H_8N_2)_3Fe^{II}]_2[Fe^{II}Mo^{V}_{12}(H_2PO_4)_6(PO_4)_2(OH)_6O_{24}]$

Atom	*x*	*Y*	*z*	*U*(eq)[a]
Mo(1)	2074(1)	826(1)	765(1)	14(1)
Mo(2)	945(1)	2110(1)	768(1)	14(1)
Fe(1)	0	0	0	14(1)
Fe(2)	3333	6667	259(1)	23(1)
P(1)	2399(1)	2318(1)	1538(1)	19(1)
P(2)	0	0	1294(1)	14(1)
O(1)	3204(2)	3143(1)	1773(1)	27(1)
O(2)	1767(2)	1729(2)	1929(1)	28(1)
O(3)	1924(1)	1866(1)	468(1)	17(1)
O(4)	1197(1)	3070(1)	500(1)	26(1)
O(8)	3014(1)	1022(1)	491(1)	25(1)
O(5)	0	0	1792(1)	29(1)
O(6)	868(1)	845(1)	1104(1)	16(1)
O(7)	1928(1)	2711(1)	1265(1)	21(1)
O(9)	2732(1)	1787(1)	1267(1)	21(1)
O(10)	58(1)	1967(1)	1221(1)	19(1)
O(11)	49(1)	1134(1)	371(1)	17(1)
N(1)	2409(2)	5628(2)	−98(1)	25(1)
N(2)	2250(2)	6372(2)	632(1)	27(1)
C(1)	2474(2)	5322(2)	−497(1)	30(1)
C(2)	1738(2)	4588(2)	−708(1)	33(1)
C(3)	915(2)	4123(2)	−496(1)	31(1)
C(4)	812(2)	4411(2)	−74(1)	26(1)
C(5)	−18(2)	3981(2)	178(1)	32(1)
C(6)	−80(2)	4321(2)	570(1)	34(1)
C(7)	665(2)	5151(2)	746(1)	30(1)
C(8)	628(3)	5589(3)	1134(1)	38(1)
C(9)	1374(3)	6401(3)	1255(1)	40(1)
C(10)	2172(2)	6777(3)	998(1)	34(1)
C(11)	1495(2)	5575(2)	507(1)	25(1)
C(12)	1573(2)	5183(2)	104(1)	24(1)

[a] *U*(eq) is defined as one-third of the trace of the orthogonalized U_{ij} tensor.

The structure of **1** was solved and refined using the SHELXTL-PLUS suite of programs (21). Observed and difference Fourier maps were used to locate the nonhydrogen atom and hydrogen atoms. For the final refinement the hydrogen atoms were placed geometrically and held in the riding mode. The last cycles of refinement included atomic positions for all the atoms, anisotropical thermal parameters for all nonhydrogen atoms. Full-matrix least-squares structure refinement against $|F^2|$ was carried out using SHELXTL-PLUS (21) package of program. The final $R1 = 0.0190$, w$R2 = 0.0468$ were obtained for a total 299 parameters. The final residuals are $\Delta\rho_{max} = 0.403$, $\Delta\rho_{min} = -0.503$ e Å^{-3}. The final atomic coordinates, selected bond distances, and angles are presented in Tables 2 and 3, respectively.

RESULTS AND DISCUSSION

The asymmetric unit, presented in Fig. 1, contains 28 and $\frac{1}{6}$ nonhydrogen atoms. There are two each of Mo (site occupancy factor (SOF) = 1.0; 1.0), Fe [SOF = 1/3 Fe(2); $\frac{1}{6}$ (Fe(1))] and P [SOF = 1 (P1); $\frac{1}{3}$ (P(2))] atoms, which are crystallographically independent. The two distinct Mo atoms are coordinated to six oxygen atoms with Mo–O distances in the range 1.665(2)–2.3057(19) Å (average Mo(1)–O = 2.009 Å and Mo(2)–O = 2.014 Å). The O–Mo–O bond angles are in the range 72.18(7)–169.39(9)°(average O–Mo(1)–O = 103.70° and average O–Mo–O = 103.52°). Of the six oxygen atoms connected to Mo, three have normal two-coordination, one is a terminal linkage and the remaining two have threefold coordination. Thus, the oxygen bond lengths show "one short–four intermediate–one long" geometry, which is unusual for molybdenum(VI) oxides. The molybdenum is connected to each other, forming the cyclic cluster of the formula $[Mo_6O_{24}]$. The two phosphorous atoms have P–O bond lengths in the range 1.501(4)–1.566(2) Å [$(P(1)–O)_{av} = 1.533$ and $(P(2)–O)_{av} = 1.541$ Å]. The O–P–O bond angles are in the range 103.84(13)–113.68(12)° [$(O–P(1)–O)_{av} = 109.38$ and $(O–P(2)–O)_{av} = 109.42°$]. The Fe(1) atom is octahedrally coordinated to six O(1) atoms

TABLE 3
Selected Bond Lengths [Å] and angles [°] for, 1, $[(C_{12}H_8N_2)_3Fe^{II}]_2[Fe^{II}Mo^{V}_{12}(H_2PO_4)_6(PO_4)_2(OH)_6O_{24}]$

Bond	Distance	Bond	Distance
Mo(1)–O(8)	1.668(2)	Mo(2)–O(4)	1.665(2)
Mo(1)–O(10)#1	1.9414(19)	Mo(2)–O(10)	1.9507(19)
Mo(1)–O(11)#1	1.9781(19)	Mo(2)–O(11)	1.9843(19)
Mo(1)–O(9)	2.0842(19)	Mo(2)–O(7)	2.0829(19)
Mo(1)–O(3)	2.097(2)	Mo(2)–O(3)	2.094(2)
Mo(1)–O(6)	2.2910(19)	Mo(2)–O(6)	2.3057(19)
Mo(1)–Mo(2)#1	2.5886(10)	Fe(1)–O(11)	2.1810(19)
P(1)–O(7)	1.506(2)	P(2)–O(5)	1.501(4)
P(1)–O(9)	1.512(2)	P(2)–O(6)	1.5539(19)
P(1)–O(1)	1.546(2)	Fe(2)–N(1)	1.982(3)
P(1)–O(2)	1.566(2)	Fe(2)–N(2)	1.986(3)
Moiety	**Angle**	**Moiety**	**Angle**
O(8)–Mo(1)–O(10)#1	105.06(9)	O(4)–Mo(2)–O(10)	105.42(10)
O(8)–Mo(1)–O(11)#1	102.39(9)	O(4)–Mo(2)–O(11)	103.48(9)
O(10)#1–Mo(1)–O(11)#1	96.21(8)	O(10)–Mo(2)–O(11)	95.71(8)
O(8)–Mo(1)–O(9)	96.93(9)	O(4)–Mo(2)–O(7)	96.97(9)
O(10)#1–Mo(1)–O(9)	84.32(8)	O(10)–Mo(2)–O(7)	86.11(8)
O(11)#1–Mo(1)–O(9)	159.79(8)	O(11)–Mo(2)–O(7)	158.14(8)
O(8)–Mo(1)–O(3)	97.06(9)	O(4)–Mo(2)–O(3)	97.99(9)
O(10)#1–Mo(1)–O(3)	156.12(8)	O(10)–Mo(2)–O(3)	155.46(8)
O(11)#1–Mo(1)–O(3)	87.60(8)	O(11)–Mo(2)–O(3)	85.74(8)
O(9)–Mo(1)–O(3)	84.18(8)	O(7)–Mo(2)–O(3)	83.83(8)
O(8)–Mo(1)–O(6)	168.74(8)	O(4)–Mo(2)–O(6)	169.39(9)
O(10)#1–Mo(1)–O(6)	84.77(8)	O(10)–Mo(2)–O(6)	83.90(8)
O(11)#1–Mo(1)–O(6)	81.60(7)	O(11)–Mo(2)–O(6)	80.19(7)
O(9)–Mo(1)–O(6)	78.33(7)	O(7)–Mo(2)–O(6)	78.35(7)
O(3)–Mo(1)–O(6)	72.44(7)	O(3)–Mo(2)–O(6)	72.18(7)
O(11)#1–Fe(1)–O(11)#4	180.00(13)	N(2)–Fe(2)–N(2)#6	91.13(11)
O(11)–Fe(1)–O(11)#5	83.91(7)	N(1)#6–Fe(2)–N(2)#2	171.95(10)
O(11)#3–Fe(1)–O(11)#5	96.09(7)	N(1)–Fe(2)–N(2)#2	93.68(10)
O(7)–P(1)–O(9)	113.68(12)	N(1)#2–Fe(2)–N(2)#2	82.33(11)
O(7)–P(1)–O(1)	105.86(12)	O(5)–P(2)–O(6)	111.53(8)

Note. Symmetry transformations used to generate equivalent atoms: #1 $-x+y, -x, z$; #2 $-y+1, x-y+1, z$; #3 $-x, -y, -z$; #4 $x-y, x, -z$; #5 $y, -x+y, -z$; #6 $-x+y, -x+1, z$.

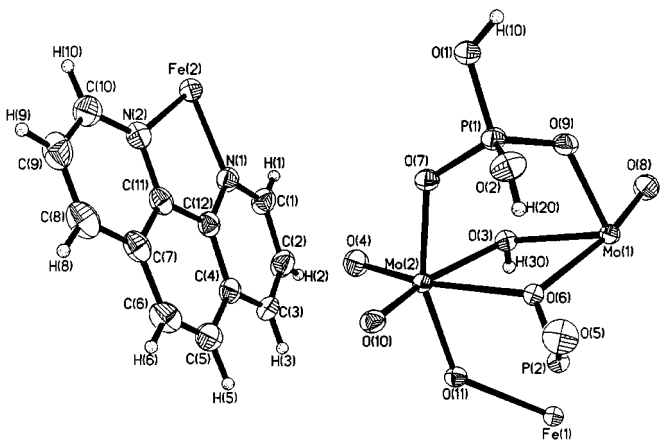

FIG. 1. ORTEP plot of **1**, $[(C_{12}H_8N_2)_3Fe^{II}]_2[Fe^{II}Mo^{V}_{12}(H_2PO_4)_6(PO_4)_2(OH)_6O_{24}]$. Thermal ellipsoids are given at 50% probability.

with equivalent bond lengths 2.1810(19) Å and three types of O–Fe–O bond angles: 83.91(7) (×6), 96.09(7) (×6), and 180.00 (×3)°. The O–Fe–O average angle is 108.0°. The Fe(2) atom is coordinated by three 1,10-phenanthroline molecules through their six nitrogen atoms with bond lengths of Fe(2)–N in the range 1.982(3) and 1.986(×3) Å and N–Fe–N bond angles in the range 82.33(11)–171.95(10)° [$(N–Fe–N)_{av} = 106.49°$], forming a distorted octahedra. The bond-strength–bond-length calculations (27, 28) and the observed geometry agree with the oxidation state of + 2 for this central Fe atom.

The structure of **1** can be considered to be built up of MoO_6, FeO_6 octahedra, and PO_4 tetrahedra linked through their vertices. The connectivity between the MoO_6 octahedra is such that it forms a cyclic cluster, Mo_6O_{24}, as shown in Fig. 2a. The cyclic clusters are connected to each other via an FeO_6 octahedra (Fig. 2b). Within the cyclic

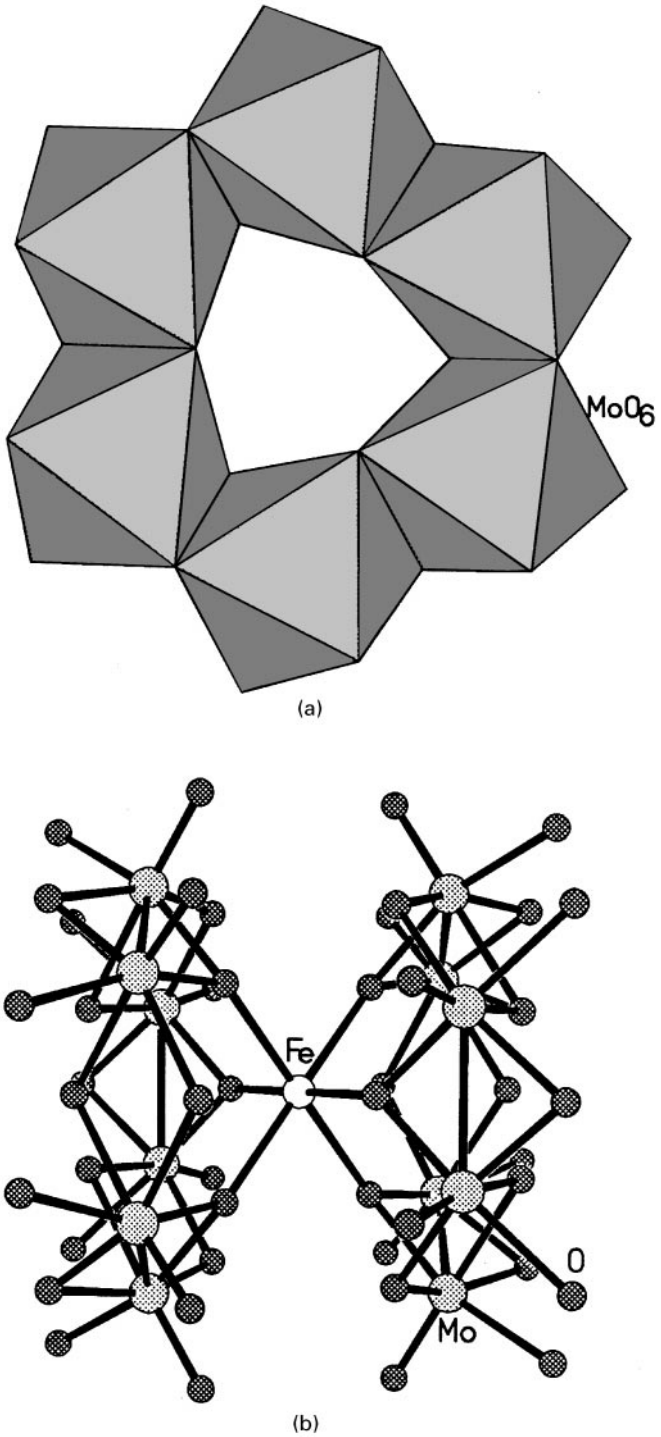

FIG. 2. (a) Polyhedral view of the cyclic Mo_6O_{24} cluster. Note that the MoO_6 octahedra share their edges. (b) The connectivity between the two such Mo–O clusters through a FeO_6 octahedra.

clusters, the MoO_6 octahedra share their edges with alternating Mo–Mo bonding distance of 2.5886(10) Å and a nonbonding distance of 3.527(8) Å. This type of connectivity is reminiscent of the Anderson structure with the central atom removed (19). This type of linkages appear to be recurrent in the rich structural chemistry of reduced oxo-molybdenum clusters and have been observed in the oxo-molybdenum phosphates (22–25). It is to be noted that identical

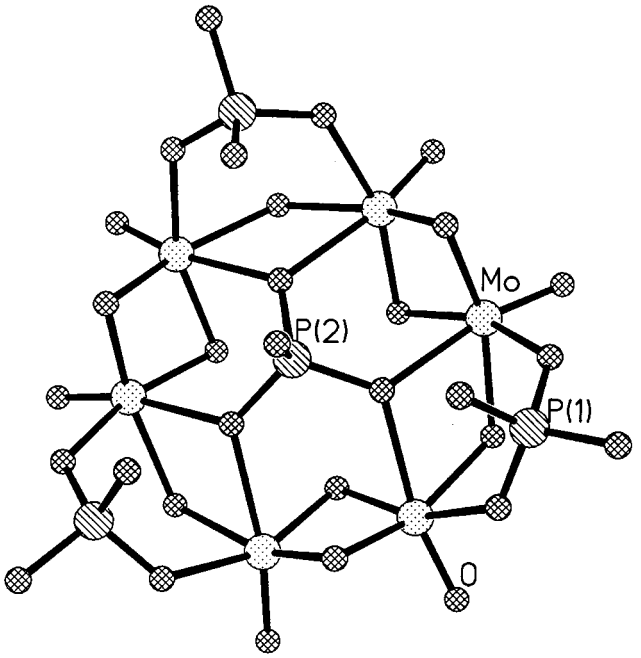

FIG. 3. Figure showing the connectivity between the cyclic cluster and the phosphate tetrahedra. Similar clusters have been observed in vanadium borates (see text).

clusters have been isolated in reduced vanadium borate systems (26).

There are two types of phosphate groups associated with this hexa-molybdenum cluster core. The central $P(2)O_4$ group is connected through three oxygen bridges with the cluster creating longer Mo···Mo distances within a pair of Mo centers. The remaining phosphate group, $P(1)O_4$, is situated near the periphery of the cluster (Fig. 3). The terminal P–OH groups on the peripheral H_2PO_4 groups are positioned as endo and exo with respect to the central P–O group. The endo P–OH group is within the hydrogen-bonding distance of the central P–O group, satisfying the band valence for the central P–O group (Fig. 3). As can be seen, the phosphate groups assume a syn conformation relative to the hexamolybdenum plane, an orientation which results in a double layer of polyhedra: one layer of tetrahedral phosphate and a second of octahedral molybdenum. One of the oxygen, O(3), which bridges the Mo(V) centers is protonated. The Fe(1) atom, which resides at the centrosymmetric site at 000 in **1**, is sandwiched between a pair of $[Mo_6(H_2PO_4)_3(PO_4)OH]_3O_{12}]^{3-}$ moieties (Fig. 2b). Similar $[M^{n+}(Mo_{12}P_8O_{62})]^{m-}$ cluster units and Mo_2 dimers with Mo–Mo single bonds near 2.6 Å have been found in a number of one-, two-, and three-dimensional reduced organic/MoPO solids (10). Bond valence sum calculations (27, 28) indicate the presence of a Mo–Mo single bond and the Mo atoms to be $+5$ oxidation state, while Fe atoms have an oxidation state of $+2$. In the counter cation, $[Fe(phen)_3]^{2+}$ complex, the Fe atom is coordinated with six nitrogen atoms of 1,10-phenanthroline.

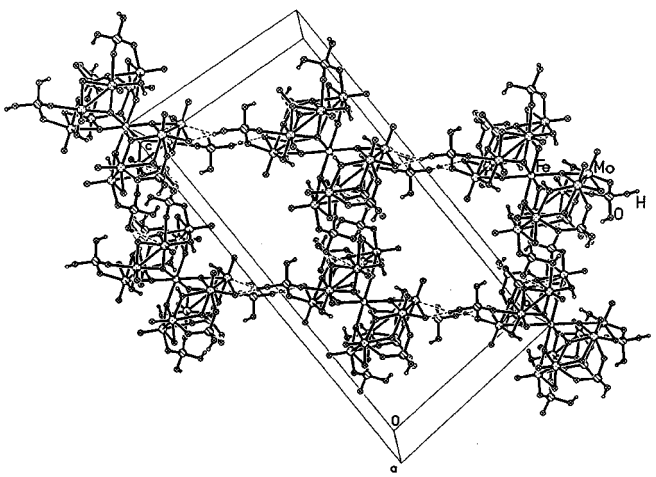

FIG. 4. Figure showing the linkages between the clusters along the *a* axis. Dotted lines represent hydrogen bond interactions. Note the formation of square channels.

The most important aspect of **1** is that the discrete cluster anions, $[FeMo_{12}(H_2PO_4)_6(PO_4)_2(OH)_6O_{24}]^{4-}$, are arranged in way to form extended architecture through hydrogen bond interactions. In Fig. 4, the cavities formed by such interactions along the *a* axis are presented. The distance between the iron atoms, Fe(1)–Fe(1), is 13.9 Å, which is large for a big molecule to reside in the middle of such cavities. The counter cation, the $Fe(phen)_3$ complex, is situated in the cavities (Fig. 5). Though the Mo_6O_{24} cluster has been known earlier (10, 15–19), the formation of this type of

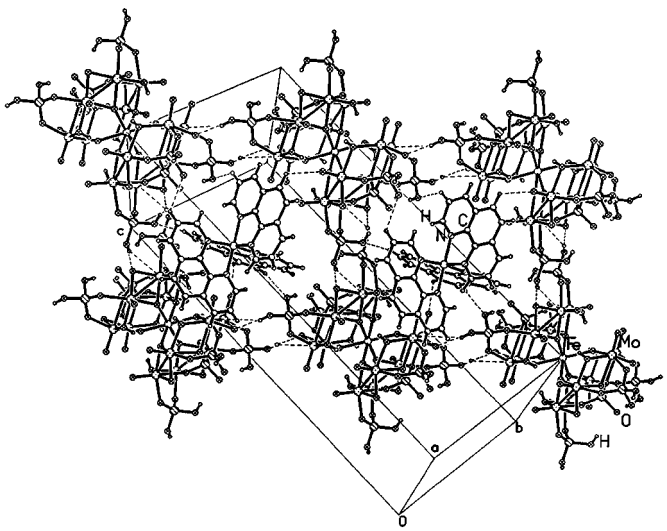

FIG. 5. Structure showing the $Fe(phen)_3$ complex in the channels. Dotted lines are possible hydrogen bond interactions.

cavity in the presence of iron has been observed for the first time. The presence of a large inorganic complex, $Fe(phen)_3$, and its interactions with the discrete cluster lends additional stability. The strong hydrogen bonds have a distance of $O(1)–H(10)\cdots O(10) = 2.644$ Å and an angle of 166°.

It is clear that the octahedral–tetrahedral molybdenum phosphate systems offer a rich crystal chemistry as exemplified by the isolation of **1**, a new type of hybrid material. Though the Mo–O cluster has been observed in many molybdenum phosphates, the isolation of such discrete cluster compounds in the presence of an iron complex enhances our understanding and possibly gives insight in the synthesis of novel structures with extended architecture. It is highly likely that similar molybdenum phosphates can also be prepared in the presence of other transition elements as well. Work on this theme is currently underway.

REFERENCES

1. A. J. Cheetham, *Science* **264,** 794 (1994), and references therein.
2. A. Clearfield, *Chem. Rev.* **88,** 125 (1988).
3. S. L. Suib, *Chem. Rev.* **93,** 803 (1993).
4. P. A. Cox, "Transition Metal Oxides." Clarendon Press, Oxford, England, 1995.
5. Y. P. Zhang, R. C. Haushalter, and A. Clearfield, *Chem. Commun.* 1055 (1996).
6. J. R. D. DeBord, R. C. Haushalter, L. A. Meyer, D. J. Rose, P. J. Zapf, and J. Zubieta, *Inorg. Chim Acta* **256,** 165 (1997).
7. J. R. Salta, Q. Chen, Y. D. Chang, and J. Zubieta, *Angew. Chem. Int. Ed. Engl.* **33,** 757 (1994).
8. M. I. Khan, Q. Chen, and J. Zubieta, *Inorg. Chim Acta* **213,** 328 (1993).
9. Y. Xu, L. H. An, and L. L. Koh, *Chem. Mater.* **8,** 814 (1996).
10. R. C. Haushalter and L. A. Mundi, *Chem. Mater.* **4,** 31 (1992) and references therein.
11. Y. Xu, B. Zhang, N. K. Goh, and L. S. Chia, *Inorg. Chim. Acta* **282,** 10 (1998).
12. K. H. Lii, Y. F. Huang, V. Zima, C. Y. Huang, H. M. Lin, Y. C. Jiang, F. L. Liao, and S. L. Wang, *Chem. Mater.* **10,** 2599 (1998) and references therein.
13. K. H. Lii and S. Boudin, *Inorg. Chem.* **37,** 799 (1998) and references therein.
14. Pamela J. Zapf, Robert P. Hammond, R. C. Haushalter, and J. Zubieta, *Chem. Mater.* **10,** 1366 (1998).
15. L. Xu, Y. Sun, E. Wang, E. Shen, Z. Liu, C. Hu, Y. Xing, Y. Lin, and H. Jia, *Inorg. Chem. Commun.* **1,** 382 (1998).
16. L. Xu, Y. Sun, E. Wang, E. Shen, Z. Liu, and C. Hu, *J. Solid State Chem.* **146,** 533 (1999).
17. L. A. Meyer and R. C. Haushalter, *Inorg. Chem.* **32,** 1579 (1993).
18. L. A. Mundi and R. C. Haushalter, *Inorg. Chem.* **31,** 3050 (1992).
19. M. T. Pope, "Heteropoly and Isopoly Oxometalates." Springer, New York, 1983.
20. A. C. T. North, D. C. Phillips, and F. S. Mathews, *Acta Crystallogr. Sect. A* **24,** 351 (1968).
21. G. M. Sheldrick, "SHELXTL-97." University of Göttingen, Germany, 1997.
22. M. I. Khan and J. Zubieta, *J. Am. Chem. Soc.* **114,** 10058 (1992).
23. Y. Xu, B. Zhang, N.-K. Goh, and L.-S. Chia, *Inorg. Chim. Acta* **282,** 10 (1998).
24. R. C. Haushalter and F. W. Lai, *Inorg. Chem.* **28,** 2905 (1989).
25. R. C. Haushalter and F. W. Lai, *Angew. Chem. Int. Ed. Engl.* **28,** 743 (1989).
26. J. T. Rijssenbeek, D. J. Rose, R. C. Haushalter, and J. Zubieta, *Angew. Chem. Int. Ed. Engl.* **36,** 1008 (1997).
27. I. D. Brown, *in* "Structure and Bonding in Crystals" (M. O'Keefe and A. Navrotsky, Eds.), Vol. II, pp. 1–30. Academic Press, New York, 1981.
28. I. D. Brown and D. Altermatt, *Acta Crystallogr. B* **41,** 24 (1985).